

New radio constraints on the obscured star formation rates of massive GRB hosts at redshifts $2 - 3.5$

PRADIP GATKINE,¹ STUART VOGEL,¹ AND SYLVAIN VEILLEUX^{1,2,3}

¹*Dept. of Astronomy, University of Maryland, College Park, MD 20742, USA*

²*Joint Space Science Institute, University of Maryland, College Park, MD 20742, USA*

³*Space Telescope Science Institute, Baltimore, MD 21218, USA*

(Received; Revised; Accepted)

Submitted to ApJ

ABSTRACT

It is not clear whether gamma-ray bursts (GRBs) are unbiased tracers of cosmic star formation at $z > 2$. Since dusty starburst galaxies are significant contributors to the cosmic star formation at these redshifts, they should form a major part of the GRB host population. However, recent studies at $z \leq 2$ have shown that the majority of the star formation activity in GRB hosts is not obscured by dust. Here, we investigate the galaxy-scale dust obscuration in $z \sim 2 - 3.5$ GRB hosts pre-selected to have high-resolution, high signal-to-noise afterglow spectra in the rest-frame ultraviolet (UV) and thus relatively low line-of-sight dust obscuration. We present new deep VLA observations of four GRB hosts, and compare the radio-based (upper limits on the) “total” star formation rates (SFRs) to the “unobscured” SFRs derived from fits to the optical-UV spectral energy distribution. The fraction of the total SFR that is obscured by dust in these galaxies is found to be $< 90\%$ in general, and $\lesssim 50\%$ for GRB 021004 and GRB 080810 in particular. These observations suggest that $z \sim 2 - 3.5$ GRBs with UV-unobscured sightlines originate in star-forming galaxies with low overall dust obscuration. By combining our results with previous studies on dark GRBs at $z > 2$, we conclude that GRB hosts do not trace the more highly dust obscured portion of the starburst population at $z > 2$.

Keywords: galaxies: evolution, high-redshift, star formation — ISM: dust, extinction

1. INTRODUCTION

Long gamma-ray bursts (GRBs) are bright bursts of gamma-rays followed by extremely luminous multi-wavelength afterglow, from the X-rays to the radio wavelengths. They have been shown to be associated with the collapse of massive stars (Hjorth et al. 2003; Stanek et al. 2003). GRBs have been observed across the cosmic history, from $z \sim 0.01$ to $z \sim 8.2$ (Tanvir et al. 2009; Salvaterra et al. 2009; Fynbo et al. 2000). These attributes make them a viable probe for tracing the star-formation history of the universe, especially at $z > 2$ where other probes are scarce.

However, the exact relation between GRB rates and cosmic star formation rate (SFR) is still an unsolved problem (Greiner et al. 2015; Schulze et al. 2015; Perley

et al. 2016a,b). Various observations of $z < 1.5$ GRB hosts have raised questions on whether GRBs can be used as unbiased tracers of star formation (Boissier et al. 2013; Perley et al. 2013; Vergani et al. 2015; Schulze et al. 2015; Perley et al. 2016b). Particularly, GRB hosts at $z < 1$ show a strong bias towards faint, low-mass ($M_* < 10^{10} M_\odot$), star-forming galaxies and lower metallicities (below solar metallicity) compared to other star-formation tracers, even after taking into account GRBs with high line-of-sight dust obscuration (Graham & Fruchter 2013; Perley et al. 2013; Kelly et al. 2014; Vergani et al. 2015; Japelj et al. 2016; Perley et al. 2016b). However, this bias appears to subside at $z > 2$ (Greiner et al. 2015) since the mean metallicity of typical star-forming galaxies is below solar. A significant amount of star formation at these redshifts happens in dusty massive starbursts (submm-bright; see Casey et al. (2014) for a review). Thus, high-mass, (relatively) metal-rich, dusty galaxies with high star formation rates may form a significant fraction of the GRB host popu-

lation at $z > 2$ (Perley et al. 2013; Greiner et al. 2016; Perley et al. 2016b). To understand whether GRBs truly trace star formation at $z > 2$, it is important to measure the total SFR (i.e. dust-obscured + dust-unobscured).

Radio observations provide a probe of recent total star formation rate. In star-forming galaxies, the radio luminosity at frequencies below a few $\times 10$ GHz is dominated by the synchrotron emission from relativistic electrons, previously accelerated by supernova remnants, propagating in the interstellar magnetic field (Condon 1992). The relativistic electrons probably have lifetimes ≤ 100 Myr, thus this component traces recent (< 100 Myr) star formation.

There are about 100 GRB host observations at radio frequencies down to limits between $3 - 500 \mu\text{Jy}$ (see Greiner et al. (2016) for details). So far, there have been 19 cm-wave observations of GRB hosts at $z > 2$, out of which two were detections: GRB 080207A and GRB 090404 (Greiner et al. 2016; Perley et al. 2013, 2015, 2016d). However, none of these high- z GRBs have high-resolution, high-SNR afterglow spectra.

GRBs with high-resolution afterglow spectra can be excellent test cases for examining the biases in GRB host population at high- z since a measure of the host metallicity may be derived from these spectra to help characterize the galaxy population traced by GRBs at $z > 2$. The availability of a high-resolution rest-frame UV spectrum of the GRB afterglow implies that the rest-frame UV is largely unobscured ($A_{UV} \lesssim 2\text{--}3$ mag). The radio observations of these GRB hosts may be used to find out whether this lack of obscuration is simply due to a clear line-of-sight or due to an overall lack of dust obscuration in the host galaxy. Dusty sightlines do not necessarily imply dusty host galaxies. This needs to be tested, especially in light of past cm-wave observations of Hatsukade et al. (2012) and Perley et al. (2013), where the deep upper limits on the radio flux from the galaxy hosts of so-called ‘dark GRBs’ (i.e. UV-dark afterglow due to high line-of-sight extinction) imply that the dark GRBs do not always occur in galaxies enshrouded by dust or in galaxies exhibiting extreme star formation rates (few $\times 100 - 1000 M_{\odot}\text{yr}^{-1}$).

New radio-based SFR constraints are particularly needed for massive ($M_{\star} \gtrsim 10^{10} M_{\odot}$) GRB hosts at $z > 2$ since the massive star-forming galaxies at high- z are likely to be significantly dusty (Casey et al. 2014; Shapley 2011). One of our objectives is therefore to understand whether massive GRB hosts at $z > 2$ share this characteristic of typical massive star-forming galaxies at $z > 2$.

This pre-selection of $z > 2$ GRB hosts based on high-resolution afterglow spectra is also useful to in-

form the total SFR of the GRB hosts in the CGM-GRB sample (Gatkine et al. 2019), particularly for the massive GRB hosts which are likely to have a substantial dust-obscured star formation component. The high-resolution spectra quantitatively trace the kinematics of the circumgalactic and interstellar media of the host. The total star formation (obscured + unobscured) is a major driver of galactic outflows that feed the circumgalactic medium (CGM). Therefore, constraining the total SFR is necessary for studying the CGM-galaxy connection.

In this paper, we report deep, late-time radio observations of four $z > 2$ GRB hosts with existing high-resolution afterglow spectra. The sample includes GRB 080810 which is the highest-redshift GRB host yet ($z = 3.35$) with deep radio observations. These results were obtained using Karl Jansky Very Large Array (VLA) in C-band ($4 - 8$ GHz). Section 2 describes the target selection, VLA observations, and analysis. In section 3, we derive the constraints on the radio-based SFRs and discuss the obscured fraction of the SFR in each GRB host individually. The implications of these results for dust obscuration in GRB hosts are discussed in Section 4 and the key conclusions are summarized in Section 5.

2. SAMPLE AND OBSERVATIONS

2.1. Sample Selection

The CGM-GRB sample is a sample of 27 $z > 2$ GRBs with high-resolution (resolving power $R > 6000$) and high signal-to-noise ratio (median SNR ~ 10) afterglow spectra (Gatkine et al. 2019). None of these GRBs have previously reported late-time radio observations. A subset of these objects is selected by imposing various criteria. Only GRBs that occurred at least six years ago are considered to ensure that the radio flux contribution from the afterglow is minimal (Perley et al. 2015). From the remaining 17, only GRB hosts with existing M_{\star} measurements and $M_{\star} > 10^{9.5} M_{\odot}$ are selected since their UV-based SFR is expected to be most affected by dust obscuration. This resulted in a set of four GRB hosts: GRB 021004, GRB 080310, GRB 080810, and GRB 121024A. Further, the VLA observations of GRB 080810 reported here (at $z = 3.35$) make it the highest-redshift GRB with a late-time radio observation of the host. Table 1 summarizes the sample and its key properties.

2.2. VLA Observations

We performed the radio observations using the fully upgraded Karl G. Jansky Very Large array (VLA) using C-band receivers spanning $4 - 8$ GHz and with a central frequency of 6 GHz. We used 3-bit samplers to

Table 1. Summary of the VLA observations

GRB ^a	z	R.A.	Dec.	Date	t_{int} (min)	Total t_{int} (min)	3σ Limit (μ Jy)	Beam size ($''$)	Flux/ bandpass	Complex gain
021004	2.323	00:26:54.68	+18:55:41.6	2018 Dec 16	120.5	270.5	3.0	3.7×4.5	3C48	J0010+1724
				2018 Dec 18	150					
				2018 Dec 04	90					
080310	2.427	14:40:13.80	−00:10:30.7	2018 Dec 11	66	402	6	3.2×4.0	3C286	J1445+0958
				2018 Dec 15	90					
				2018 Dec 18	90					
				2018 Dec 24	66					
080810	3.35	23:47:10.49	+00:19:11.5	2018 Dec 09	71	343	3.8	3.7×4.9	3C48	J2323-0317
				2018 Dec 22	135					
				2019 Jan 05	71					
				2019 Jan 10	66					
121024A	2.298	04:41:53.30	−12:17:26.6	2018 Dec 17	123	123	18	3.9×5.6	3C138	J0437-1844

^aAll the observations were performed in the C-band (4 – 8 GHz) in C array configuration of the VLA

utilize the entire 4096 MHz bandwidth of the C band to maximize the continuum sensitivity. The dual polarization setup was used. The observations were conducted in the C array configuration during the months of December 2018 to January 2019 (program VLA 18B-312, PI: Gatkine). The integration time for each GRB host is listed in Table 1 (typical ~ 4.5 hours). A nearby complex gain (amplitude and phase) calibrator was observed every 30 – 40 minutes during any scheduling block and a standard flux calibrator was observed every hour. The $3\text{-}\sigma$ rms and the synthesized beam size for each source are listed in Table 1.

The data reduction was carried out using the Common Astronomy Software Applications package (CASA) version 5.5.0. The standard CASA pipeline was used to flag and calibrate the observations. Imaging and deconvolution was performed using the `tclean` function in CASA. Natural weighting was employed while cleaning the measurement sets to maximize the continuum sensitivity. In the case of GRB 121024A, additional flagging was performed to clip the outlier visibilities and channels heavily affected with radio frequency interference. Further, self-calibration was performed to clean the image around a bright source at a separation of $6'$, a robust weighting was employed, and a multi-term multi-frequency synthesis (mtmfs, with 2 terms) deconvolver was used to account for spectral index gradient in the much brighter contaminating source.

The synthesized beam size for C-configuration observations is significantly coarser (beam size $\sim 4''$) than the angular extent of the galaxy (1 kpc translates to \sim

$0.1''$ at $z \sim 2.5$). Therefore, the host galaxies are unresolved and can be treated as point sources here. The 1σ flux-density level was derived by sampling a blank region spanning $\sim 100 \times$ synthesized beam area around the target.

The maps for GRB 021004 and GRB 080810 have rms sensitivities close to that predicted by the VLA noise calculator. However, GRB 121024A and GRB 080310 had particularly bright sources near the half-power response of the primary beam. At this location in the primary beam, the amplitude response is variable owing to antenna pointing errors, which result in amplitude gain errors in the visibilities that are a function of field position in addition to antenna, frequency, and time. Standard self-calibration does not work well if there are position-dependent errors; antenna pointing errors limited the dynamic range of the maps for GRB 080310 and especially GRB 121024A, and consequently our sensitivity for these objects.

3. RADIO- AND UV-BASED SFR

3.1. Radio-based SFR

As described in Section 1, the radio continuum at frequencies below a few $\times 10$ GHz traces the total (i.e. dust-obscured + dust-unobscured) star formation activity in the last 100 Myr (Condon 1992). The radio-far-IR relation for star-forming galaxies which quantifies the radio-SFR relation is shown to hold true at intermediate and high redshifts (Sargent et al. 2010). On the other hand, the UV/optical light (including the emission lines) primarily probes the portion of the SFR that is

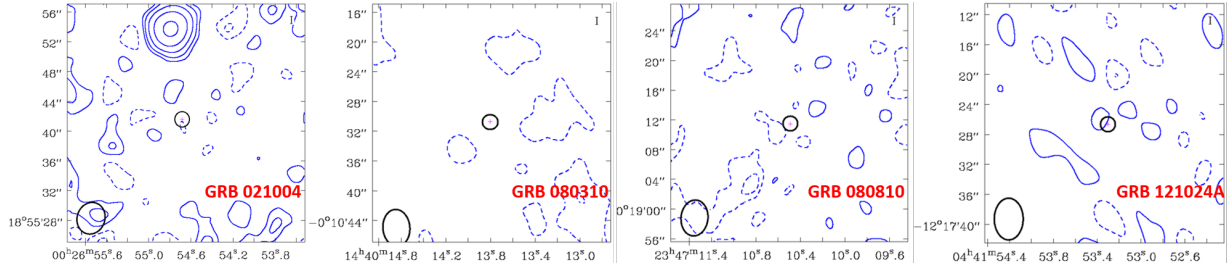


Figure 1. Contour maps of the radio flux density in $30'' \times 30''$ fields centered on the four GRBs of our sample. The location of the GRB and $2''$ error circle are marked as red crosses and black circles, respectively. The synthesized beam is shown in the bottom left corner. The contours are marked as $-12, -6, -3, -1.5, 1.5, 3, 6, 12 \times \sigma$ with negative values marked as dotted contours. None of the GRB hosts are detected at the 3σ level.

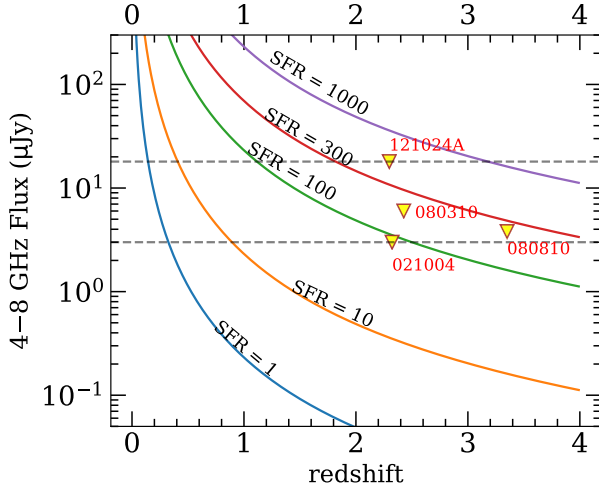


Figure 2. Curves showing the radio flux density averaged over 4–8 GHz for various star formation rates (M_{\odot}/yr) over a redshift range $z \sim 0 - 4$ using a spectral index of $\alpha = 0.7$. The 3σ upper limits of various GRBs are shown with downward triangles. The horizontal dotted lines are drawn to guide the eye.

not significantly obscured by dust (i.e. dust-unobscured SFR) even with dust attenuation included in the modeling (see the example of GRB 100621A in Stanway et al. 2014). Thus, a significant discrepancy between the UV-based and radio-based SFR measures would imply the presence of substantial dust obscuration within the galaxy. In the discussion below, we use the following naming system:

SFR_{total}: Radio-based total SFR

SFR_{unobscured}: UV-based unobscured SFR,

SFR_{obscured}: the portion of SFR that is obscured due to the dust ($= \text{SFR}_{\text{total}} - \text{SFR}_{\text{unobscured}}$).

Here, we observe the GRB hosts in C-band (4–8 GHz) at $z \sim 2 - 3.5$, thus we are sensitive to $\nu_{\text{rest}} = 25 \pm 10$ GHz. The rest-frame radio luminosity is produced by three mechanisms: non-thermal synchrotron emission (ϵ_1), free-free emission (ϵ_2), and thermal emission from

dust (ϵ_3), as shown in Yun & Carilli (2002). The thermal dust component is insignificant ($< 1\%$) at the frequencies of interest. The radio-SFR relation for star-forming galaxies (Yun & Carilli 2002) is thus given by:

$$S(\nu_{\text{obs}}) = (\epsilon_1 + \epsilon_2 + \epsilon_3) \times \frac{(1+z)\text{SFR}}{D_L^2} \quad (1)$$

where,

$$\epsilon_1 = 25 f_{\text{nth}} \nu_0^{-\alpha}$$

$$\epsilon_2 = 0.71 \nu_0^{-0.1}$$

$$\epsilon_3 = 1.3 \times 10^{-6} \frac{\nu_0^3 [1 - e^{-(\nu_0/2000)^\beta}]}{e^{0.048 \nu_0 / T_d - 1}}.$$

Here, the symbols ϵ_1 , ϵ_2 , and ϵ_3 represent the contributions from non-thermal synchrotron, free-free, and dust thermal emission respectively. D_L is luminosity distance in Mpc, SFR is star formation rate in $M_{\odot}\text{yr}^{-1}$, ν_0 is rest-frame frequency in GHz, f_{nth} is the scaling factor, α is the synchrotron spectral index, T_d is the dust temperature in K, and β is the dust emissivity. For the typical values of T_d (~ 60 K) and β (1.35), the dust emission is insignificant for $\nu_{\text{rest}} \sim 25$ GHz. hence, we neglect this term. The non-thermal synchrotron emission is the most dominant contributor in the given frequency range. Since we do not have a robust measurement of the actual spectral index for any of our objects, we assume a canonical average value of $\alpha = -0.7$. Past literature has used values ranging from -0.6 to -0.75 (Hatsukade et al. 2012; Perley et al. 2013, 2015; Stanway et al. 2014; Greiner et al. 2016). This range of α affects the radio luminosity by 25%. This equation assumes a Salpeter initial mass function (IMF). Due to various assumptions in the calibration of radio-based SFRs, it is subject to a systematic uncertainty of about a factor of ~ 2 (Yun & Carilli 2002; Bell 2003; Murphy et al. 2011).

Figure 2 shows the observed flux densities averaged over 4–8 GHz for various star formation rates as a function of redshift and the respective 3σ upper limits of our targets. The UV- and radio-derived SFRs for our four targets are summarized in Table 2 along with

the stellar masses and ratios of radio-based (total) and UV-based (dust-unobscured) SFRs.

3.2. Late-time afterglow emission

The GRBs have long-lived radio afterglows. Therefore, any estimates of SFR using the radio emission can only be made after the afterglow has faded considerably to ensure minimal/no contamination due to the afterglow. We compiled the past early-time radio observations of the afterglows of our target GRBs available in the literature and extrapolated the afterglow decay using a canonical long GRB radio light curve model (forward shock model) with a t^{-1} decay (Chandra & Frail 2012) as follows:

$$f(t) = \begin{cases} F_m t_m^{-1/2} t^{1/2}, & \text{if } t < t_m. \\ F_m t^{-1}, & \text{if } t > t_m. \end{cases} \quad (2)$$

Here, F_m is the peak flux density at a given frequency and t_m is the time of the peak in that frequency. For this extrapolation, we used a conservative approach. We use the latest flux density measurement in C-band (if available) as the peak flux density. If it is not available (eg: GRB 121024A), we extrapolate the flux density using the standard GRB radio afterglow model described in Chandra & Frail (2012). The typical values of t_m range between rest-frame 3 and 6 days at a rest-frame frequency of ~ 25 GHz (which we probe since our targets are at $z \sim 2 - 3.5$). We translate this t_m to the observer frame for each GRB and plot the radio afterglow evolution in Figure 3. The three lines show the decay with $t_m = 3, 4.5$, and 6 days (in the rest frame). No early-time radio observations are available for GRB 080310. The conservative approach used here gives the upper limit of radio flux density due to the afterglow and further shows that the late-time radio fluxes for our observations are dominated by the host galaxy and are not likely to be contaminated by the afterglow.

3.3. SFR in each GRB host

We summarize the UV-derived and radio-derived SFRs for the four GRBs in the following subsections. Using the VLA observations, we obtain an estimate of the total SFR ($\text{SFR}_{\text{total}}$), independent of assumptions on the dust extinction (in the line of sight or otherwise). We also compare the observed ratio $\text{SFR}_{\text{total}}/\text{SFR}_{\text{unobscured}}$ for our GRB hosts with the same ratio for star-forming galaxies with a similar stellar mass at a redshift range $z \sim 2 - 2.5$, as derived from the CANDELS survey (Whitaker et al. 2017) and summarize this in Figure 4.

3.3.1. GRB 021004

GRB 021004 is one of the best studied GRBs from the gamma-rays to radio wavelengths. The optical afterglow was detected 3.2 minutes after the prompt high-energy emission and was followed up extensively (Fynbo et al. 2005). The extremely blue host galaxy of GRB 021004 was identified and studied through late-time imaging in the rest-frame UV and optical bands. HST ACS imaging in the F606W band revealed that the host galaxy has a very compact core with a half-light radius of only 0.4 kpc (at $z = 2.323$). The impact parameter of the afterglow position is only $0.015''$, corresponding to a distance of 119 pc, which is one of the smallest for long GRBs (Fynbo et al. 2005; Blanchard et al. 2016). The line-of-sight extinction A_V is 0.20 ± 0.02 mag. (using the SMC extinction law) as derived after 1 week of afterglow decay (Fynbo et al. 2005). The Ly α -derived neutral hydrogen column density (N_{HI}) along the line of sight is modest ($\sim 10^{19} \text{ cm}^{-2}$; Prochaska et al. 2008b).

Castro-Tirado et al. (2010) derived the host SFR of $40 \text{ M}_{\odot} \text{ yr}^{-1}$ (without any dust correction) by attributing all of the H α emission to star formation. Given the small A_V , the dust correction was assumed to be minimal from the afterglow SED. On the other hand, Jakobsson et al. (2005) have estimated a lower limit of SFR as $10.6 \text{ M}_{\odot} \text{ yr}^{-1}$ by converting the Ly α flux to SFR (Kennicutt 1998) and assuming a 100% Ly α escape fraction.

We derive a 3σ upper limit on the C-band flux density of $3.0 \text{ } \mu\text{Jy}$, corresponding to a radio SFR limit of $85 \text{ M}_{\odot} \text{ yr}^{-1}$ at $z \sim 2.323$. This result is consistent with the low A_V derived from the optical-NIR SED and therefore suggests that the host galaxy as a whole is not significantly affected by dust. This observation identifies a galaxy that is able to sustain a SFR of $\sim 40 \text{ M}_{\odot} \text{ yr}^{-1}$ at $z \sim 2.3$ without significant dust obscuration. Using the non-extinction-corrected H α emission, we get $\text{SFR}_{\text{unobscured}} = 40 \text{ M}_{\odot} \text{ yr}^{-1}$, so the ratio $\text{SFR}_{\text{total}}/\text{SFR}_{\text{unobscured}}$ is < 2.1 for this $M_* > 10^{10} \text{ M}_{\odot}$ galaxy. In contrast, the corresponding ratio derived for the main sequence of star-forming galaxies at $z \sim 2.5$ from Whitaker et al. (2017) is ~ 6 .

Given the small impact parameter of the afterglow (119 pc) from the centroid of the galaxy, the apparent lack of significant dust extinction along the line of sight to the GRB, and in the host galaxy as a whole from the radio observations, is puzzling.

3.3.2. GRB 080310

The afterglow of GRB 080310 was detected 1.5 minutes after the prompt high-energy emission and was followed up extensively (see Littlejohns et al. 2012, for a full discussion). The redshift of this GRB is 2.427 (Prochaska et al. 2008a; Vreeswijk et al. 2008). Perley

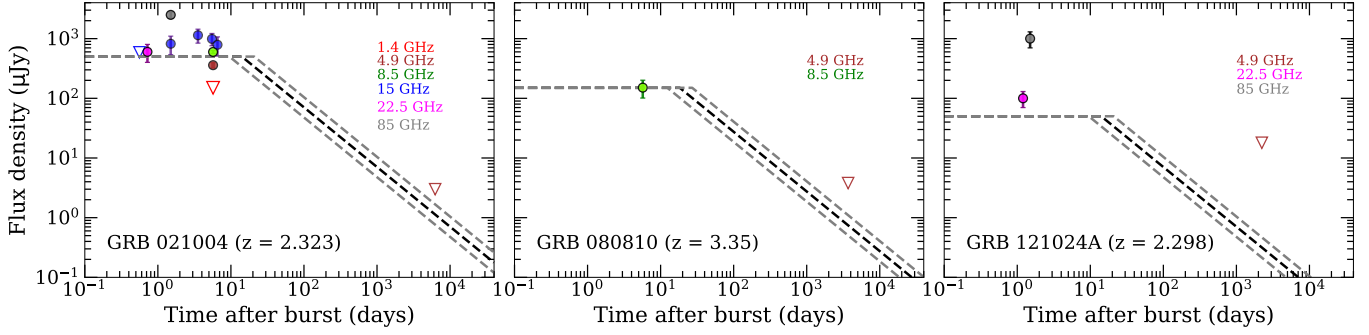


Figure 3. Radio evolution of the afterglows of GRB 021004, GRB 080810, and GRB 121024A, extrapolated using the canonical afterglow evolution model described in Section 3.1.

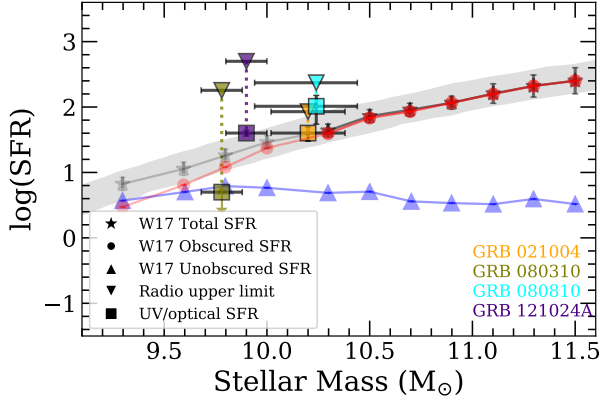


Figure 4. The SFR – M_* relation decomposed into total (black star), obscured (red circle), and unobscured components (blue triangle) of the star formation rate for the galaxies in the CANDELS survey at $z \sim 2 - 2.5$ (Whitaker et al. 2017). The gray band corresponds to the typical 0.3 dex width of the observed relation. Individual GRBs in our sample are shown in various colors with their UV-derived SFR (tracing the dust-unobscured SFR) and the radio-derived SFR (tracing the total SFR).

et al. (2008) estimated a low line-of-sight extinction A_V of 0.10 ± 0.05 mag. using an SMC-like extinction law (at an average time of $t_0 + 1750$ s). The line-of-sight N_{HI} is modest ($\sim 10^{18.8} \text{ cm}^{-2}$).

The late-time host galaxy imaging using the Low Resolution Imaging Spectrometer (LRIS) on the Keck-I telescope yielded a non-detection with a g-band limiting magnitude of 27.0 (Perley et al. 2009). We estimate a SFR upper limit of $4.5 \text{ M}_\odot \text{ yr}^{-1}$ using the UV luminosity-SFR relation for GRB host galaxies described in Savaglio et al. (2009). Perley et al. (2016b) estimated $\log(M_*/M_\odot) = 9.8 \pm 0.1$ using *Spitzer* 3.6 μm imaging. However, we caution the reader of the possibility that the *Spitzer* 3.6 μm flux is contaminated by the diffraction spike from a nearby star despite careful modeling and subtraction of the spike (Perley et al. 2016b).

The VLA observations constrain the SFR to less than $180 \text{ M}_\odot \text{ yr}^{-1}$ ($3\text{-}\sigma$ upper limit). However, this limit is

not sufficiently deep to constrain the dust obscuration in the host galaxy of GRB 080310.

3.3.3. GRB 080810

This is the highest-redshift GRB in our sample at $z = 3.35$. The afterglow of GRB 080810 was detected 80 seconds after the prompt emission by the X-ray telescope (XRT; Burrows et al. (2005)) and UV-optical telescope (UVOT; Roming et al. (2005)) on board the Neil Gehrels Swift Observatory (Gehrels et al. 2004). Prochaska et al. (2008a) obtained the optical spectra of the afterglow using the Keck HIRES spectrograph starting 37 minutes after the trigger and derived a redshift of 3.35. The Ly α -derived line-of-sight N_{HI} is small ($\sim 10^{17.5} \text{ cm}^{-2}$). We refer the readers to Page et al. (2009) for a discussion of the extensive multi-wavelength follow-up of this GRB.

Extensive late-time ground-based photometry and spectroscopy of the host galaxy of GRB 080810 revealed an extended structure with a bright compact region (see Wiseman et al. 2017, for more details). Further, a strong detection of redshifted Ly α emission at a redshift of 3.36 confirmed the association of the GRB and the detected host galaxy (Wiseman et al. 2017). They estimate a modest host extinction of $A_V \sim 0.4$ mag. from SED fitting. Greiner et al. (2015) convert the extinction-corrected UV luminosity to SFR (using the $L_{\text{UV}} - \text{SFR}$ relation in Duncan et al. (2014) and $A_{1600} \sim 1.3$ mag.) to obtain $\text{SFR} \sim 100 \text{ M}_\odot \text{ yr}^{-1}$, which is further corroborated by SED fitting (Wiseman et al. 2017). The uncorrected SFR is $\sim 30 \text{ M}_\odot \text{ yr}^{-1}$. The stellar mass, derived from the *Spitzer* 3.6 μm photometry, is $\log(M_*/M_\odot) = 10.2 \pm 0.1$ (Perley et al. 2016c).

Here we report the first ever deep late-time radio observation of a GRB with a spectroscopic redshift $z > 3.1$. We derive a $3\text{-}\sigma$ upper limit on the C-band flux density of $3.8 \mu\text{Jy}$, corresponding to a radio-based SFR upper limit of $235 \text{ M}_\odot \text{ yr}^{-1}$ at $z \sim 3.35$. The dust-corrected SFR from the UV SED is therefore consistent with the total SFR limit derived from the radio observations. This

further implies that the modest A_V estimated from the UV SED fitting reasonably takes into account the dust correction.

Using the uncorrected UV SFR, we derive a ratio $\text{SFR}_{\text{total}}/\text{SFR}_{\text{unobscured}} < 7$ for this $M_* > 10^{10} M_\odot$ galaxy. This is consistent with the corresponding ratio derived for the main sequence of star-forming galaxies at $z \sim 2 - 2.5$ from Whitaker et al. (2017), which again gives $\text{SFR}_{\text{total}}/\text{SFR}_{\text{unobscured}} \sim 6$. However, if the dust-corrected UV SFR ($\sim 102 M_\odot \text{yr}^{-1}$) is used instead, we get $\text{SFR}_{\text{radio}}/\text{SFR}_{\text{UV,corr}} < 2.3$. Here, we extrapolate the non-evolution of this ratio from $z \sim 2.5$ to 3.3 for the star-forming galaxies on the main sequence at a given M_* , as presented in Whitaker et al. (2017).

3.3.4. GRB 121024A

The afterglow of GRB 121024A was followed up 93 seconds after the prompt emission by the X-ray telescope (XRT; Burrows et al. (2005)) on board the Neil Gehrels Swift Observatory (Gehrels et al. 2004). Tanvir et al. (2012) obtained the optical/NIR spectra of the afterglow using the X-shooter spectrograph on the Very Large Telescope (VLT) and determined a redshift of 2.298. The line-of-sight N_{HI} of $10^{21.5} \text{ cm}^{-2}$ indicates that this is a damped $\text{Ly}\alpha$ system. We refer the readers to Friis et al. (2015) for a detailed summary of the extensive multi-wavelength follow-up of this GRB.

Various emission lines including $\text{H}\alpha$, $\text{H}\beta$, $[\text{O II}] \lambda\lambda 3727, 3729$ doublet, $[\text{N II}] \lambda 6583$, and $[\text{O III}] \lambda\lambda 4959, 5007$ were detected in the X-shooter NIR spectrum of the afterglow. Extensive optical and NIR photometry of the host galaxy was obtained using VLT/HAWK-I, NOT, and GTC (see Friis et al. 2015, for details). The stellar population synthesis modelling of the host yielded a modest extinction A_V of 0.15 ± 0.15 mag. and $\log(M_*/M_\odot) = 9.9^{+0.2}_{-0.3}$.

Friis et al. (2015) estimate the SFR from the extinction-corrected $\text{H}\alpha$ and $[\text{O II}]$ fluxes as 42 ± 11 and $53 \pm 15 M_\odot \text{yr}^{-1}$ using conversion factors from Kennicutt (1998). However, note that the extinction correction to the SFR is small ($\sim 15\%$). They further corroborate this SFR by stellar population synthesis modelling.

The $3\text{-}\sigma$ upper limit on the C-band flux density of GRB 121024A is $18 \mu\text{Jy}$. The relatively higher background is due to a bright source at $6'$ angular separation. Using the VLA observations, we obtain a $3\text{-}\sigma$ upper limit of the total SFR as $500 M_\odot \text{yr}^{-1}$. However, this limit is not sufficiently deep to constrain the dust obscuration in the host galaxy of GRB 121024A. The limiting $\text{SFR}_{\text{total}}/\text{SFR}_{\text{unobscured}} < 12.5$ is consistent with the corresponding expected ratio (~ 5) from Whitaker et al.

(2017) for a star-forming galaxy of this stellar mass on the main sequence at $z \sim 2 - 2.5$.

4. DISCUSSION

Our observations have targeted massive ($M_* > 10^{9.5} M_\odot$) high- z GRBs ($z \sim 2 - 3.5$) with high-resolution and high SNR rest-frame UV afterglow spectra (i.e. a rest-frame UV-bright afterglow). The results presented here, in concert with previous observations for the so-called ‘dark’ GRBs (rest-frame UV/optically dark afterglows; Perley et al. 2013, 2015; Greiner et al. 2016), show that the fraction of dust-obscured star formation ($\text{SFR}_{\text{obscured}}/\text{SFR}_{\text{total}}$) in most of the GRB hosts (even at $z > 2$) is less than 90% (with a few exceptions such as GRB 090404; Perley et al. 2013). There is no evidence for extreme dust obscuration in the star-forming regions of GRB host galaxies, within the uncertainties of the radio flux–SFR relation. This result is summarized in Figures 4 and 5.

The two best-constrained cases of GRB 021004 ($z = 2.323$) and GRB 080810 ($z = 3.35$) show that the radio-based total SFR $\lesssim 2 \times$ UV-based unobscured SFR. Further, the ratio of total-to-unobscured SFRs for these GRB hosts is significantly smaller than the corresponding ratio for the star-forming galaxies on the main sequence (Whitaker et al. 2017).

Particularly, GRB 021004 provides a striking example of lack of significant dust obscuration in the central region of a star-forming galaxy at $z > 2$, given that the separation of the GRB from the galaxy centroid is only 119 pc (Chen 2012). The sightline extinction, derived from the afterglow is also small ($A_V = 0.2 \pm 0.02$ mag.). Two possible scenarios can explain these results: a) the GRB occurred in a locally dusty cloud but globally, the host galaxy lacks significant amount of dust. The low sightline extinction would then imply that the burst occurred along a clear sightline within its star-forming cloud. b) the GRB occurred in a star-forming region which has cleared the dust from past star formation and the overall galaxy also lacks significant amount of dust. The GRB sightline would then be a representative sightline. Similarly, for GRB 080810 ($z = 3.35$), the deep radio limit suggests that the overall star formation activity in this GRB host is not heavily obscured by dust, and possibly even less obscuration than the star-forming main sequence at $z = 3.35$ (Speagle et al. 2014; Whitaker et al. 2017).

The limits in our observations are 3 times deeper than the previous limits on the SFR at $z > 2$ (Perley et al. 2015), and thus provide tighter constraints on whether GRB hosts at these redshifts are more likely to be dusty starburst galaxies or not. The results from our limited

Table 2. Summary of GRB host properties

GRB ^a	z	$\log(N_{\text{HI}})^a$ (cm^2)	M_* (M_\odot)	SFR_{UV} ($M_\odot \text{ yr}^{-1}$)	$\text{SFR}_{\text{Radio}}^b$ ($M_\odot \text{ yr}^{-1}$)	$\frac{\text{SFR}_{\text{total}}}{\text{SFR}_{\text{UV}}}$
021004	2.323	19.00 ± 0.2^c	10.2 ± 0.18^g	40 ± 10	< 85	< 2.1
080310	2.427	18.80 ± 0.1^d	9.78 ± 0.2^h	< 5	< 180	—
080810	3.35	17.5 ± 0.15^e	10.24 ± 0.1^h	102 ± 48	< 235	< 2.3
121024A	2.298	21.5 ± 0.1^f	$9.9^{+0.2f}_{-0.3}$	40 ± 4	< 500	< 12.5

^aLy α -derived N_{HI} ^b 3σ upper limit, ^cProchaska et al. (2008b), ^dFox et al. (2008), ^ePage et al. (2009), ^fFriis et al. (2015), ^gSavaglio et al. (2009), ^hPerley et al. (2016b)

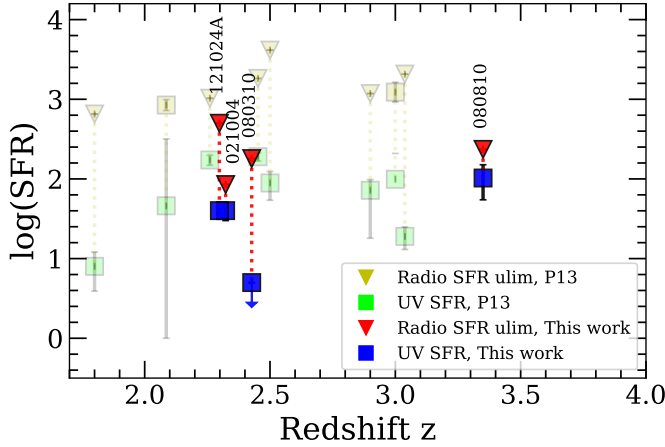


Figure 5. The comparison of the radio-derived SFR (tracing the total SFR) and UV-derived SFR (tracing the dust-unobscured SFR) as a function of redshift for the four GRBs presented here (in the foreground), and GRBs in the literature in the background. P13: Perley et al. (2013) and one data point (GRB 060814) from Greiner et al. (2016).

sample suggest that the GRBs with UV-bright afterglows (i.e. optically thin sightlines in UV) at $z \sim 2-3.5$ are likely to be star-forming galaxies with SFRs moderately higher ($< 5\times$) than the star-forming main sequence (Speagle et al. 2014), but without significant dust obscuration in their star-forming regions.

However, it is possible that this result only applies to the GRBs with UV-bright afterglows due to our selection criteria. At the same time, the dust extinction along a sightline may not necessarily represent the dust obscuration on a galaxy scale, for optically thin as well as optically thick sightlines (in UV). More radio observations of GRB hosts at $z > 2$ with a depth at least $2 \times \text{SFR}_{\text{UV}}$ are necessary to confirm this hypothesis. This is required for GRBs with UV-bright afterglows as well as with UV/optically dark afterglows to rule out any selection bias based on the line-of-sight extinction.

5. SUMMARY

If the GRBs are unbiased tracers of star formation at high redshifts ($z > 2$), then we should expect that a large fraction of GRB hosts are highly dust-obscured starbursting galaxies, since these are well known to be major contributors to the cosmic star formation at high redshifts. The goal of our study was to investigate the galaxy-scale dust obscuration in the GRB hosts with optically thin sightlines in the UV. We conducted deep radio observations of a subset of four massive ($M_* > 10^{9.5} M_\odot$) GRB hosts at $z > 2$ for which high signal-to-noise (typical SNR ~ 10) and high-resolution ($\Delta v < 50 \text{ km s}^{-1}$) rest-frame UV spectra of the afterglow are available. The selected targets are GRB 021004, GRB 080310, GRB 080810, and GRB 121024A. We measured the total SFR (= obscured + unobscured SFR) of the hosts using VLA C-band observations and compared them against the unobscured component of the SFR, measured from UV-optical photometry. The depth of the radio observations in this study has allowed us to put tight constraints on the ratio of the total-to-unobscured SFRs ($\text{SFR}_{\text{total}}/\text{SFR}_{\text{unobscured}}$).

We find that the radio-based star formation rates are in general not substantially higher than those obtained from the optical/UV measurements. Thus, the fraction of total star formation that is obscured by dust ($\text{SFR}_{\text{obscured}}/\text{SFR}_{\text{total}}$) in most of the GRB hosts, even at $z > 2$, is less than 90%. Particularly, for the two best-constrained objects, GRB 021004 ($z = 2.323$) and GRB 080810 ($z = 3.35$), we find that the upper limit of the radio-based ‘total SFR’ is less than twice the UV-based ‘unobscured SFR’ of the GRB hosts (thus, $\text{SFR}_{\text{obscured}}/\text{SFR}_{\text{total}} < 50\%$). Our results suggest that the dust obscuration in the star-forming regions of these galaxies is small, and sometimes (e.g. for GRB 021004 and GRB 080810) even smaller than the dust obscuration seen in typical main-sequence star-forming galaxies at these redshifts.

The present upper limits on the radio-based SFRs prevent us from determining where the GRB host population lies with respect to the main sequence of star-forming galaxies at $z > 2$. Deeper radio observations to a depth of $2 \times \text{SFR}_{\text{UV}}$ are required to answer this question.

P.G. was supported by NASA Earth and Space Science Fellowship (ASTRO18F-0085) for this research. The authors are grateful to Drs. S. Bradley Cenko and Daniel Perley for their useful comments in the early

stages of this paper. We thank Dr. Ashley Zauderer and Nicholas Ferraro for helpful discussions about data analysis. The National Radio Astronomy Observatory is a facility of the National Science Foundation operated under cooperative agreement by Associated Universities, Inc.

Facilities: VLA

Software: CASA (McMullin et al. 2007), astropy (Robitaille et al. 2013)

REFERENCES

- Bell, E. F. 2003, *The Astrophysical Journal*, 586, 794
- Blanchard, P. K., Berger, E., & Fong, W.-f. 2016, *The Astrophysical Journal*, 817, 144
- Boissier, S., Salvaterra, R., Le Floch, E., et al. 2013, *Astronomy & Astrophysics*, 557, A34
- Burrows, D. N., Hill, J., Nousek, J. A., et al. 2005, *Space science reviews*, 120, 165
- Casey, C. M., Narayanan, D., & Cooray, A. 2014, *Physics Reports*, 541, 45
- Castro-Tirado, A. J., Møller, P., García-Segura, G., et al. 2010, *Astronomy & Astrophysics*, 517, A61
- Chandra, P., & Frail, D. A. 2012, *The Astrophysical Journal*, 746, 156
- Chen, H.-W. 2012, *Monthly Notices of the Royal Astronomical Society*, 419, 3039
- Condon, J. 1992, *Annual review of astronomy and astrophysics*, 30, 575
- Duncan, K., Conselice, C. J., Mortlock, A., et al. 2014, *Monthly Notices of the Royal Astronomical Society*, 444, 2960
- Fox, A. J., Ledoux, C., Vreeswijk, P. M., Smette, A., & Jaunsen, A. O. 2008, *Astronomy & Astrophysics*, 491, 189
- Friis, M., De Cia, A., Krühler, T., et al. 2015, *Monthly Notices of the Royal Astronomical Society*, 451, 167
- Fynbo, J., Holland, S., Andersen, M., et al. 2000, *The Astrophysical Journal Letters*, 542, L89
- Fynbo, J. P. U., Gorosabel, J., Smette, A., et al. 2005, *The Astrophysical Journal*, 633, 317
- Gatkine, P., Veilleux, S., & Cucchiara, A. 2019, *The Astrophysical Journal*, 884, 66
- Gehrels, N., Chincarini, G., Giommi, P., et al. 2004, *The Astrophysical Journal*, 611, 1005
- Graham, J., & Fruchter, A. 2013, *The Astrophysical Journal*, 774, 119
- Greiner, J., Fox, D. B., Schady, P., et al. 2015, *The Astrophysical Journal*, 809, 76
- Greiner, J., Michałowski, M. J., Klose, S., et al. 2016, *Astronomy & Astrophysics*, 593, A17
- Hatsukade, B., Hashimoto, T., Ohta, K., et al. 2012, *The Astrophysical Journal*, 748, 108
- Hjorth, J., Sollerman, J., Møller, P., et al. 2003, *Nature*, 423, 847
- Jakobsson, P., Björnsson, G., Fynbo, J., et al. 2005, *Monthly Notices of the Royal Astronomical Society*, 362, 245
- Japelj, J., Vergani, S., Salvaterra, R., et al. 2016, *Astronomy & Astrophysics*, 590, A129
- Kelly, P. L., Filippenko, A. V., Modjaz, M., & Kocevski, D. 2014, *The Astrophysical Journal*, 789, 23
- Kennicutt, R. C. 1998, *Annual Review of Astronomy and Astrophysics*, 36, 189
- Littlejohns, O., Willingale, R., O'Brien, P., et al. 2012, *Monthly Notices of the Royal Astronomical Society*, 421, 2692
- McMullin, J., Waters, B., Schiebel, D., Young, W., & Golap, K. 2007, in *Astronomical data analysis software and systems XVI*, Vol. 376, 127
- Murphy, E., Condon, J., Schinnerer, E., et al. 2011, *The Astrophysical Journal*, 737, 67
- Page, K. L., Willingale, R., Bissaldi, E., et al. 2009, *Monthly Notices of the Royal Astronomical Society*, 400, 134
- Perley, D., Bloom, J., & Li, W. 2008, *GRB Coordinates Network*, 7406
- Perley, D., Levan, A., Tanvir, N., et al. 2013, *The Astrophysical Journal*, 778, 128
- Perley, D., Perley, R., Hjorth, J., et al. 2015, *The Astrophysical Journal*, 801, 102
- Perley, D., Krühler, T., Schulze, S., et al. 2016a, *The Astrophysical Journal*, 817, 7
- Perley, D., Tanvir, N. R., Hjorth, J., et al. 2016b, *The Astrophysical Journal*, 817, 8
- . 2016c, *The Astrophysical Journal*, 817, 8

- Perley, D. A., Hjorth, J., Tanvir, N. R., & Perley, R. A. 2016d, *Monthly Notices of the Royal Astronomical Society*, stw2789
- Perley, D. A., Cenko, S., Bloom, J., et al. 2009, *The Astronomical Journal*, 138, 1690
- Prochaska, J., Foley, R., Holden, B., et al. 2008a, *GRB Coordinates Network*, 7397
- Prochaska, J. X., Dessauges-Zavadsky, M., Ramirez-Ruiz, E., & Chen, H.-W. 2008b, *The Astrophysical Journal*, 685, 344
- Robitaille, T. P., Tollerud, E. J., Greenfield, P., et al. 2013, *Astronomy & Astrophysics*, 558, A33
- Roming, P. W., Kennedy, T. E., Mason, K. O., et al. 2005, *Space Science Reviews*, 120, 95
- Salvaterra, R., Della Valle, M., Campana, S., et al. 2009, *Nature*, 461, 1258
- Sargent, M. T., Schinnerer, E., Murphy, E., et al. 2010, *The Astrophysical Journal Supplement Series*, 186, 341
- Savaglio, S., Glazebrook, K., & Le Borgne, D. 2009, *The Astrophysical Journal*, 691, 182
- Schulze, S., Chapman, R., Hjorth, J., et al. 2015, *The Astrophysical Journal*, 808, 73
- Shapley, A. E. 2011, *Annual Review of Astronomy and Astrophysics*, 49, 525
- Speagle, J. S., Steinhardt, C. L., Capak, P. L., & Silverman, J. D. 2014, *The Astrophysical Journal Supplement Series*, 214, 15
- Stanek, K. Z., Matheson, T., Garnavich, P., et al. 2003, *The Astrophysical Journal Letters*, 591, L17
- Stanway, E. R., Levan, A. J., & Davies, L. J. 2014, *Monthly Notices of the Royal Astronomical Society*, 444, 2133
- Tanvir, N., Fynbo, J., Melandri, A., et al. 2012, *GRB Coordinates Network*, Circular Service, No. 13890, # 1 (2012), 13890
- Tanvir, N. R., Fox, D. B., Levan, A., et al. 2009, *Nature*, 461, 1254
- Vergani, S., Salvaterra, R., Japelj, J., et al. 2015, *Astronomy & Astrophysics*, 581, A102
- Vreeswijk, P., Jakobsson, P., Jaunsen, A., & Ledoux, C. 2008, *GRB Coordinates Network*, 7391
- Whitaker, K. E., Pope, A., Cybulski, R., et al. 2017, *The Astrophysical Journal*, 850, 208
- Wiseman, P., Perley, D., Schady, P., et al. 2017, *Astronomy & Astrophysics*, 607, A107
- Yun, M. S., & Carilli, C. 2002, *The Astrophysical Journal*, 568, 88